HHS Public Access

Author manuscript

Cell Metab. Author manuscript; available in PMC 2017 March 30.

Published in final edited form as:

Cell Metab. 2016 March 08; 23(3): 467–478. doi:10.1016/j.cmet.2016.02.003.

The Circadian Clock in the Ventromedial Hypothalamus Controls Cyclic Energy Expenditure

Ricardo Orozco-Solis[1,3], **Lorena Aguilar-Arnal**[1], **Mari Murakami**[1], **Rita Peruquetti**[1], **Giorgio Ramadori**[2], **Roberto Coppari**[2], and **Paolo Sassone-Corsi**[1,*]

[1]Center for Epigenetics and Metabolism, Unite 904 INSERM, Department of Biological Chemistry, University of California, Irvine, Irvine, California 92697 [2]Universite de Geneve, CMU Departement Phyme, rue Michel Servet 1, 1211 Geneva, Switzerland

Abstract

Organismal homeostasis relies on coherent interactions among tissues, specifically between brain-driven functions and peripheral metabolic organs. Hypothalamic circuits compute metabolic information to optimize energetic resources, but the role of the circadian clock in these pathways remains unclear. We have generated mice with targeted ablation of the core-clock gene *Bmal1* within Sf1-neurons of the ventromedial hypothalamus (VMH). While this mutation does not affect the central clock in the suprachiasmatic nucleus (SCN), the VMH clock controls cyclic thermogenesis in brown adipose tissue (BAT), a tissue that governs energy balance by dissipating chemical energy as heat. VMH-driven control is exerted through increased adrenergic signaling within the sympathetic nervous system, without affecting the BAT's endogenous clock. Moreover, we show that the VMH circadian clock computes light and feeding inputs to modulate basal energy expenditure. Thus, we reveal a previously unsuspected circuit where an SCN-independent, hypothalamic circadian clock controls BAT function, energy expenditure and thermogenesis.

Graphical abstract

*Corresponding author: psc@uci.edu.

[3]Present address: National Institute of Genomic Medicine (INMEGEN), Mexico city, Mexico

AUTHORS CONTRIBUTION

ROS Designed research, performed experiments, analyzed data and contributed to the writing of the manuscript. LAA, performed experiments and revised the manuscript. MM, RP, performed experiments. GR, RC, provided reagents. PSC, Designed and directed research, wrote and revised the manuscript.

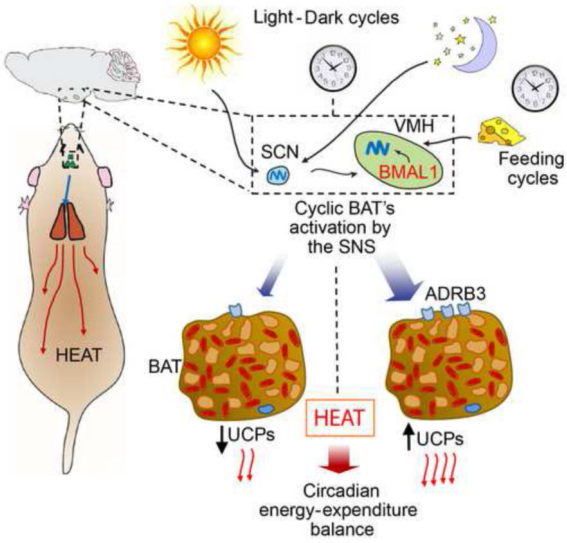

INTRODUCTION

Homeostasis in mammals is achieved through a variety of highly sophisticated mechanisms that control the balance between energy intake and expenditure (Myers and Olson, 2012). A key feature of homeostatic regulation is its intrinsic cyclic nature, which is in large part controlled by circadian rhythms. The intimate interplay between nutrition, metabolism, exercise and circadian physiology involves the molecular clock, a complex molecular machinery present in virtually every cells and tissues of an organism (Asher and Sassone-Corsi, 2015).

At the molecular level, the circadian clock consists on a network of interlocked transcriptional– translational feedback loops. Core molecular gears are the transcription factors CLOCK and BMAL1, which heterodimerize and bind E-box promoter elements on the genome, activating a large number of clock-controlled genes (CCGs) (Orozco-Solis and Sassone-Corsi, 2014). Disruption of the circadian clock has been linked to development of metabolic diseases. For example, in humans, short sleep duration and altered feeding time are associated to development of metabolic unbalances (Buxton et al., 2012), while in rodents the disruption of the circadian clock also triggers metabolic disturbances (Masri and Sassone-Corsi, 2013). Importantly, tissue-specific ablation of BMAL1 as a single core clock protein causes drastic physiological consequences illustrating its distinct functions within a given tissue. For example, BMAL1 ablation in the adipose tissue provokes obesity in mice and a shift in the diurnal rhythm of food intake (Paschos et al., 2012); in hepatocytes causes the reduction of the detoxification capacity (Johnson et al., 2014). Finally, BMAL1 controls the alternate cycles of dormancy and proliferation in epidermal stem cells so to keep the skin-tissue homeostasis (Janich et al., 2011). Thus, the circadian role of BMAL1 is tightly linked to central metabolic functions of cells and tissues.

Circadian physiology, metabolism and behavior are generated by a multitude of clocks that operate in concert to insure homeostasis (Buijs and Kalsbeek, 2001; Masri and Sassone-

Corsi, 2013). In mammals, the central clock resides in the suprachiasmatic nucleus of the hypothalamus (SCN), which receives and translates light signaling originated at retinal neurons and transmitted through the retinohypothalamic tract (RHT). While various clocks in peripheral tissues have been characterized, the presence of clocks in other brain areas has been proposed but not convincingly demonstrated. Specifically, a food-entrainable oscillator and a metamphetamine-entranable oscillator have been postulated (Honma and Honma, 2009) and their location hypothesized in other hypothalamic nuclei, including arcuate nucleus (ARC), ventromedial (VMH) and dorsomedial hypothalamus (DMH). The functional significance and autonomy of these non-SCN brain clocks, as well as their physiological interactions with the SCN and peripheral clocks, remain largely elusive.

Hypothalamic nuclei, including the paraventricular nucleus (PVN), the ARC, the DMH, the VMH and the lateral hypothalamus (LH), govern energy balance via both metabolic and behavioral responses (Myers and Olson, 2012). Particularly, the VMH is thought to have a role in controlling food intake and peripheral metabolism (Dhillon et al., 2006; Myers and Olson, 2012). The steroidogenic factor 1 (SF1) is essential for development of VMH neurons, and in the brain, SF1 is expressed specifically in the VMH (Choi et al., 2013). Importantly, SF1 neurons within the VMH govern distinct aspects of glucose metabolism through dedicated signaling pathways involving regulators and nutrient sensors including, PI3K, leptin and insulin receptors, SOCS3, SIRT1, FOXO1, and SF1 itself. Moreover, the VMH is also implicated in the modulation of energy expenditure through the thermogenesis process, and SF1 neurons appear to be necessary for regulation of diet-induced thermogenesis (Amir, 1990; Kim et al., 2011; Minokoshi et al., 1986; Perkins et al., 1981).

Because of the intimate connections between the circadian clock, cellular metabolism and organismal homeostasis, we generated a mouse model with a brain nucleus-specific, SCN-independent, disruption of the clock by *Bmal1* ablation in SF1 neurons of the VMH. We show that the circadian clock in the VMH significantly contributes to the control of energy balance through the modulation of the metabolic rate and the circadian activity of the brown adipose tissue (BAT). Our findings also reveal that in a context where the SCN clock is intact, another hypothalamic nucleus rhythmically and specifically governs a central homeostatic function such as energy expenditure.

RESULTS

Targeting the VMH clock by ablation of the *Bmal1* gene in SF1 neurons

To explore a possible role of the circadian pacemaker in specialized non-SCN hypothalamic neurons, we generated mice lacking the core clock gene *Bmal1* specifically in the SF1 neurons of the VMH. To do so, we bred mice homozygous for the conditional *Bmal1*$^{loxP/loxP}$ allele (Storch et al., 2007) with mice expressing *Cre* recombinase under the control of the promoter from the steroidogenic factor 1 (*Sf1*) gene (*Sf1-Cre* mice), whose expression is restricted to the VMH-specific SF1 neurons (Dhillon et al., 2006) (Figure 1A). To verify the excision of the *Bmal1* gene in the VMH, we compared *Bmal1*$^{loxP/loxP}$ mice with littermate mice *Bmal1*$^{loxP/loxP}$ carrying one copy of the *Sf1-Cre* recombinase transgene (*Sf1-Cre*, *Bmal1*$^{loxP/loxP}$). Specific ablation was validated by targeted PCR from micro-dissected VMH and other brain areas such as SCN and total hippocampus (Figures 1A and 1B). Next

we performed immunohistochemistry (IHC) analyses in brain slices using anti BMAL1-specific antibodies. The number of BMAL1-positive cells in the VMH of the *Sf1-Cre*, *Bmal1*$^{loxP/loxP}$ mice was drastically reduced when compared to the *Bmal1*$^{loxP/loxP}$ littermates (Figures 1C and 1D). Importantly, BMAL1 protein levels in adjacent hypothalamic nuclei, the SCN and the DMH, remained unaltered, confirming the VMH-specific ablation of *Bmal1* (Figures 1C and 1D). We further validated the deletion by monitoring *Bmal1* expression in total RNA from micro-dissected ARC, VMH and SCN nuclei, and total hippocampus. *Bmal1* expression was significantly decreased exclusively in the VMH of *Sf1-Cre*, *Bmal1*$^{loxP/loxP}$ mice (Figure 1E). Thus, *Bmal1* ablation is restricted to the VMH and does not alter BMAL1 expression in other adjacent nuclei.

As BMAL1 is a core component of the circadian clock, we sought to determine if targeted ablation of *Bmal1* in the SF1-neurons affects the circadian oscillator both in the VMH and in the SCN. While *Bmal1, Per1* and *Per2* circadian expression in the VMH is virtually abolished in the *Sf1-Cre*, *Bmal1*$^{loxP/loxP}$ mice (Figure 1F and Table S1), their circadian expression in the SCN remained unaltered, (Figure 1G and Table S1). In line with previous studies (Storch et al., 2007), ablation of BMAL1 results in increased *Cry1* expression in the VMH, while no effect is observed in the SCN (Figures 1F, 1G and Table S1). Thus, a clock intrinsic to the VMH directs circadian gene expression within SF1 neurons while its function does not influence the central pacemaker in the SCN.

The VMH clock regulates cyclic energy expenditure

The VMH is thought to control metabolic homeostasis and energy balance (Bingham et al., 2008; Choi et al., 2013; Dhillon et al., 2006; Kim et al., 2012; Kim et al., 2011; Klockener et al., 2011; Ramadori et al., 2011; Yadav et al., 2009; Zhang et al., 2008). Remarkably, mice with reduced BMAL1 in the SF1 neurons display a sustained decrease in weight of ~10% when compared with *Bmal1*$^{loxP/loxP}$ littermates (Figure 2A). This difference is not due to an increase in daily caloric intake or alteration in the pattern of time of feeding (Figure 2B). Moreover, there are no substantial differences in the total ambulatory activity (Figure 2C), suggesting that the decrease in body weight in the *Sf1-Cre*, *Bmal1*$^{loxP/loxP}$ mice might appear as a consequence of altered energy expenditure.

To assess the cause of lower body weight in *Sf1-Cre,Bmal1*$^{loxP/loxP}$ mice, we measured the energy expenditure by indirect calorimetry (Virtue and Vidal-Puig, 2013). In line with the observed lower body weight, *Sf1-Cre*, *Bmal1*$^{loxP/loxP}$ mice presented altered respiration shown by higher rates in oxygen consumption (VO_2), (Figure 2D; light $P > 0.05$, dark $P < 0.05$, ANCOVA) and carbon dioxide production (VCO_2), (light $P > 0.05$, dark $P < 0.05$, ANCOVA) (Figure 2E). Consequently, *Sf1-Cre*, *Bmal1*$^{loxP/loxP}$ mice showed increased energy expenditure (EE) (light $P > 0.05$, dark $P < 0.05$ ANCOVA) (Figure 2F; Table S2). Importantly, these effects on respiration rate are mostly restricted to the dark period (Figures 2D-2F). Under light-dark conditions, no statistically significant increase in the circadian acrophase was found (Figure 2G).

It has been established that the VMH modulates energy expenditure through thermoregulatory responses (Amir, 1990; Kim et al., 2011). Thereby, we sought to determine daily fluctuation in body temperature that in the mouse is known to decrease during the

resting (Iight) phase and peak during the active (dark) phase (Figure 2H) (Gerhart-Hines et al., 2013; Shiromani et al., 2004). Interestingly, *Sf1-Cre*, *Bmal1*$^{loxP/loxP}$ mice presented significantly higher rectal temperature from ZT 12 to ZT 16 (Figure 2H). Thermographic imaging confirmed these results and identified the highest thermal point in correspondence to the brown adipose tissue (BAT) (Figures 2I and 2J). Collectively, these results reveal that the VMH clock influences thermal oscillations in BAT.

BAT over-activation during the active phase

Growing evidence in rodents and humans illustrate the active role of BAT on energy expenditure and thermoregulation by dissipating chemical energy as heat (Ruan et al., 2014). In this context, our findings reveal that *Sf1-Cre*, *Bmal1*$^{loxP/loxP}$ mice show increased circadian metabolic rate and temperature mainly during the dark period. To establish whether the observed phenotype may be due to disrupted function of the circadian clock within the BAT, we determined circadian gene expression of clock and thermogenic genes in this tissue. Importantly, the circadian clock in brown adipocytes is not altered, as indicated by the normal oscillations of the clock genes *Bmal1*, *Per2*, *Cry1*, *Nr1d1* (*Reverbα*) and *Rorα* (Figure 3A, Table S3), showing that the increased nocturnal temperature in *Sf1-Cre*, *Bmal1*$^{loxP/loxP}$ mice is independent of the core clock present in BAT. Next, we analyzed the circadian expression of genes involved in parasympathetic signaling, fatty acid utilization, mitochondrial regulation and thermogenesis. Interestingly, β-adrenergic receptor 3 (*Adrb3*) expression shows a marked increase at ZT16, suggesting an activation of the adrenergic signaling in BAT during the dark period in the mutant mice (Figure 3B). Consistently, a parallel overexpression profile is common to genes promoting fatty acid oxidation such as the fatty acid binding protein 3 (*Fabp3*) and the rate-controlling enzyme of the longchain fatty acid beta-oxidation, the carnitine palmitoyltransferase c (*Cpt1b*) (Figure 3B)(Cypess et al., 2015; Plaisier et al., 2012). Furthermore, expression of the nuclear respiratory factor 1 (*Nrf1*), a key transcription factor regulating nuclear-encoded mitochondrial genes, also displayed significantly higher amplitude at ZT16 (Figure 3B)(Wu et al., 1999). Finally, all three genes encoding the uncoupling proteins UCP1, UCP2 and UCP3 are upregulated in the mutant mice, mostly during the active phase (Figure 3B). The uncoupling proteins UCP1-3 are critically involved in thermogenesis as they transform chemical energy into heat by uncoupling the respiratory chain from ATP synthesis (Cannon and Nedergaard, 2004).

Histological analysis of the BAT by hematoxylin and eosin staining reveals smaller lipid droplets and higher tissue density in the *Sf1-Cre*; *Bmal1*$^{loxP/loxP}$ mice as compared to the control littermates (H&E; Figure 4A). Lipid content visualization using oil-red-O showed reduced staining on the BAT from *Sf1-Cre*, *Bmal1*$^{loxP/loxP}$ mice, further confirming morphological differences (Figure 4A). Also, we observed a reduced cell area in BAT adipocytes from the *Sf1-Cre, Bmal1*$^{loxP/loxP}$ mice (Figure 4A). Moreover, we found decreased levels of free fatty acids (FFA), the main fuel for mitochondrial β-oxidation, in the *Sf1-Cre*; *Bmal1*$^{loxP/loxP}$ mainly during the dark period (Figure 4B). Thus, the VMH clock influences energy expenditure modulating the physiology and function of brown adipocytes.

The significant effect of the VMH-specific ablation of BMAL1 prompted us to investigate the expression of BAT functional genes in *Bmal1*$^{loxP/loxP}$ as compared to the *Sf1-Cre*,

Bmal1$^{loxP/loxP}$ mutants during the dark period. Interestingly, we found increased expression of the BAT-specific genes *Zicl* and *Epsti1* at ZT16 (Figure 4C). On the other hand, expression of genes participating in the regulation of BAT activity by increasing mitochondrial biogenesis and fatty acid oxidation (Cederberg et al., 2001; Harms and Seale, 2013) were drastically induced in the BAT of *Sf1-Cre*; *Bmal1*$^{loxP/loxP}$ mice (Figure 4C). These included Forkhead box protein C2 (*Foxc2*), Peroxisome proliferator-activated receptor alpha (*Pparα*), Peroxisome proliferator-activated receptor gamma coactivator 1-alpha (*Pgc1a*), *Nrf1*, and Type II iodothyronine deiodinase (*Dio2*). Next, we analyzed the expression of genes directly implicated in the control of catabolic pathways responsible for heat production, and found significant induction in the BAT from *Sf1-Cre*; *Bmal1*$^{loxP/loxP}$ mice on *Ucp1*, *Ucp2* and *Ucp3* genes (Figure 4D). We also confirmed a consistent increase on PPARα protein levels, a master positive regulator of uncoupling proteins gene expression and energy expenditure (Barbera et al., 2001; Fan and Evans, 2014; Mandard et al., 2004) (Figure 4E). Brown adipocytes utilize not only fatty acids, but also glucose as extra source of energy to produce heat (YU et al., 2002). Accordingly, an increase on *Fabp3*, *Cpt1b* and the glucose transporter 4 (*Glut4*) gene expression was observed in *Sf1-Cre*, *Bmal1*$^{loxP/loxP}$ mice, suggesting that both, the glucose and fatty acid oxidation are potentiated in the mutant mice (Figure 4D). Altogether, these results strongly support a scenario in which mitochondrial activity in the *Sf1-Cre*, *Bmal1*$^{loxP/loxP}$ mice is elevated. To directly prove this possibility, we quantified the mitochondrial (mtDNA) copy number and its relative activity from isolated BAT. We found a remarkable increase in mtDNA in the *Sf1-Cre*; *Bmal1*$^{loxP/loxP}$ when compared with their *Bmal1*$^{loxP/loxP}$ littermates (Figure 4F). Accordingly, the protein levels of the mitochondrial protein marker mtCO1 was also elevated in the *Sf1-Cre*;*Bmal1*$^{loxP/loxP}$ mice (Figure 4F). To determine mitochondrial activity, we measured β-oxidation rates and mitochondrial oxidative capacity in BAT explants. Importantly, we found a pervasive induction of fatty acid oxidation in the *Sf1-Cre*, *Bmal1*$^{loxP/loxP}$ mice (Figure 4G). This was accompanied by increased and more localized MitoTracker signal (Figure 4H), and increased green signal as revealed by JC-1 staining (Figure S1A) thereby revealing higher mitochondrial density and a decrease in the mitochondrial polarization within the BAT from the *Sf1-Cre*, *Bmal1*$^{loxP/loxP}$ mice (Özbudak et al., 2010). It is generally accepted that BAT mitochondria have an increased proton conductance as a result of higher UCP1 activity (Stuart et al., 1999). To determine whether proton leak is potentiated in *Sf1-Cre*; *Bmal1*$^{loxP/loxP}$ mice, we measured its rate in the BAT from these mice. *Sf1-Cre*; *Bmal1*$^{loxP/loxP}$ mice displayed a distinct tendency for higher proton leak in the BAT when compared to *Bmal1*$^{loxP/loxP}$ mice (Figure S1B). Collectively, these findings demonstrate that the BAT from Sf1-cre;*Bmal1*$^{loxP/loxP}$ is expending more energy through two main pathways: 1) An increment in mitochondrial biogenesis, 2) An increased capacity to transform chemical energy into heat during the dark period.

Clock-driven BAT activation via the sympathetic nervous system

In humans and rodents, BAT thermogenesis is controlled centrally by the sympathetic nervous system (SNS) through activation of β3 adrenoreceptors (β3-AR, encoded by *Adrb3*) in brown adipocytes (Amir, 1990; Cypess et al., 2015; Kim et al., 2011; Morrison et al., 2014). Also, the VMH is thought to control BAT activation and thermogenesis (Halvorson et al., 1990; Lopez et al., 2010; Martinez de Morentin et al., 2014; Morrison et al., 2014).

Importantly, *Adrb3* expression levels are significantly increased in BAT from *Sf1-Cre*,*Bmal1*$^{loxP/loxP}$ mice (Figure 4D), suggesting the implication of the SNS-BAT pathway in increased thermogenic capacity of these mice (Liew et al., 2013). To test this hypothesis, mice were intraperitoneally injected with the selective ADRB3 antagonist SR592030A at ZT16 and the thermogenic capacity was assessed by evaluating temperature, fatty acid oxidation and gene expression responses (Bexis and Docherty, 2009; Ootsuka et al., 2011). To do so, we first determined the effect of SR59230A at 1, 2 and 4 hours post-injection in *Bmal1*$^{loxP/loxP}$ mice. Time-dependent effects on the rectal temperature and β-oxidation from BAT explants were most effective 1hr post injection (Figures S2A and S2B). Notably, expression of thermogenic genes closely paralleled the systemic effects, with specific genes slightly delayed. (Figures S2C and S2D), confirming that the thermogenic capacity could be best assessed at ~1.5 hours post SR59230A injection. We found that blocking the ADRB3 signaling by the selective antagonist significantly reduces the body temperature in both mice groups, however the effect was significantly stronger in the *Sf1-Cre*, *Bmal1*$^{loxP/loxP}$ than in the *Bmal1*$^{loxP/loxP}$ mice ($P < 0.05$, *t*-test Figure 5A; Table S4). Importantly, consumption of chemical energy is also differentially affected by ADRB3 blockage as revealed by increased reduction in fatty acid oxidation efficiency from *Sf1-Cre*, *Bmal1*$^{loxP/loxP}$ mice ($P < 0.05$, *t*-test, Figure 5B; Table S4). In line with these results, there is a more pronounced decrease in expression of genes participating in heat production (*Ucp1*, *Ucp2*, *Ucp3*), fatty acid catabolic pathways (*Cpt1b*, *Fabp3*) and the glucose transporter *Glut4* (Figure 5C; Table S4). Importantly, the effect of SR59230A on the expression of key mitochondrial regulatory genes such as *Nrf1*, *Pgc1α* and *Pparα* was also more pronounced in the *Sf1-Cre*, *Bmal1*$^{loxP/loxP}$ mice (Figure 5C; Table S4).

Next, we compared the thermogenic response to 5 hours cold exposure (4° C) by measuring body temperature and *Ucp1* expression in BAT. While both mice groups showed the same reduction in body temperature after 6 hours, the *Sf1-Cre*, *Bmal1*$^{loxP/loxP}$ mice maintain higher temperature ($P < 0.05$, Twoway ANOVA)(Figure 5D) during the dark period. This response is reflected by the increase in gene expression of thermogenic genes *Nrf1*, *Cpt1b*, *Ucp1* and *Ucp2* (Figure 5E-5H). Collectively, these results demonstrate that: 1) the *Sf1-Cre*, *Bmal1*$^{loxP/loxP}$ mice show a remarkably high ADRB3 activation through the SNS, which in turns leads to higher stimulation of BAT with subsequent effects on gene expression, fatty acid consumption and heat production; 2) At 4 °C, the *Sf1-Cre*, *Bmal1*$^{loxP/loxP}$ mice show higher thermogenic response during the dark period, as compared to their *Bmal1*$^{loxP/loxP}$ littermates.

Marginal control of the WAT by the VMH Clock

Chronic β3 adrenergic stimulation induce browning of the white adipose tissue (WAT). Our results show that the BAT on the *Sf1-Cre*, *Bmal1*$^{loxP/loxP}$ mice is sympathetically over-stimulated, particularly during the dark period. This notion prompted us to evaluate whether the WAT may be also stimulated, inducing browning in this tissue (Nedergaard and Cannon, 2014). To test this hypothesis we analyzed the genetic profile of WAT and beige markers in the inguinal WAT (Harms and Seale, 2013; Kajimura et al., 2010). Analysis of key genes implicated in the activation of beige tissue revealed no or little increase of their expression (Figure S3A). Similarly, expression of thermogenic genes (*Cpt1b*, *Fabp3*, *Adrb3*, *Ucp1* and

Ucp2) was not altered in the mutant mice (Figure S3A). Furthermore, histological analyses also show lack of morphological differences in the WAT of both genotypes (Figure S3B). In the same line, mtDNA and free fatty acid content at ZT 4 and ZT 16 was not affected (Figures S3C and S3D). Finally, we analyzed the expression of beige and WAT markers in the subcutaneous white adipose tissue (scWAT), and no significant differences between the *Sf1-cre/Bmal1*$^{loxP/loxP}$ and the *Bmal1*$^{loxP/loxP}$ mice could be observed (Figure S3E). This scenario is in line with the notion that the BAT is the primary sympathetically stimulated tissue, while induction of the WAT is effective solely in extreme conditions, such as chronic cold exposure or by compensatory browning on the WAT elicited by pausing the BAT by genetic or surgical BAT-SNS denervation (Nedergaard and Cannon, 2014; Schulz et al., 2013). These results show that the thermogenic pathways and browning in WAT are weakly stimulated in the *Sf1-Cre*, *Bmal1*$^{loxP/loxP}$ mice, confirming that lack of BMAL1 in the VMH specifically impinges the function of BAT. Finally, ablation of *Bmal1* in the VMH does not lead to significant changes in liver gene expression (Figure S4).

The VMH clock modulates basal diurnal metabolic rate

Our findings indicate that the VMH internal clock plays a role in the control of peripheral circadian rhythms. Interestingly, previous studies have suggested that external zeitgebers such as light or feeding may alter the VMH's internal clock (Kozlov et al., 2007; Orozco-Solis et al., 2015). Therefore, to determine whether the lack of BMAL1 in Sf1 neurons affects circadian behavior in the absence of external zeitgebers, mice were exposed to 12:12 hr LD cycles followed by constant darkness (DD) with food available *ad-libitum*. Interestingly, there is a more pronounced, significant shortening in the length of the free running period (tau value, τ) in the *Sf1-Cre,Bmal1*$^{loxP/loxP}$ compared with the *Bmal1*$^{loxP/loxP}$ mice (23.85 ± 0.02512, 23.77 ± 0.02904, respectively $P < 0.05$ *t*-test, Figure 6A). Thus, the behavioral circadian rhythms are less robust in the mutant mice in absence of external zeitgebers. We also analyzed circadian respiratory rhythms by indirect calorimetry in constant darkness. Paralleling the results on circadian behavior, circadian respiratory profile is significantly different of about 4 hrs in the acrophase of O_2 consumption, CO_2 and heat production ($P < 0.01$ *t*-test) in the *Sf1-Cre*, *Bmal1*$^{loxP/loxP}$ mice when compared with the *Bmal1*$^{loxP/loxP}$ littermates after 50 days in DD (Figure 6B). The mutant mice maintain an increased fluctuation of their respiratory and energy expenditure rates, as reflected by the values, amplitude and MESOR on LD or DD in *ad-libitum* feeding conditions (Figure S5). As the VMH has been implicated in nutrient sensing (Orozco-Solis et al., 2015), we sought to determine whether the zeitgeber properties of restricted feeding would trigger changes in the circadian respiratory rhythms under LD and DD conditions in *Sf1-Cre,Bmal1*$^{loxP/loxP}$ mice. As expected, restricted feeding powerfully synchronizes the respiratory rhythm to the meal-time as shown by the peak on the respiratory rate at ZT 13-17 (Figure 6C). Interestingly, while *Bmal1*$^{loxP/loxP}$ animals on restricted feeding and DD were also re-synchronized with a peak at the beginning of feeding time, *Sf1-Cre,Bmal1*$^{loxP/loxP}$ mice presented a significant phase delay at the end of the meal period ($P < 0.05$ *t*-test) (Figure 6D). Moreover, under these conditions the *Sf1-Cre,Bmal1*$^{loxP/loxP}$ show resilience in matching their respiratory rate with the feeding condition, maintaining a moderate increase on the global energy expenditure as revealed by the amplitude and MESOR (Figure S5). Collectively these results imply that: 1) The circadian clock in the Sf1 neurons is able to

compute light-dark cycles information to modulate the respiratory rate timing 2) Both light-dark cycles and feeding restriction act as external zeitgebers to modulate the respiratory rate. Therefore, our results show that the circadian clock in the SF1 neurons modulates rhythms of circadian energy expenditure and concomitantly can be modulated by external zeitgebers.

DISCUSSION

A number of studies in both humans and rodents have illustrated that disruption of circadian rhythms is tightly linked to metabolic disorders and unbalance of energy metabolism (Buxton et al., 2012; Chaix et al.; Eckel-Mahan and Sassone-Corsi, 2013; Eckel-Mahan et al., 2013), though the regulatory circuits and signaling mechanisms have remained poorly understood.

The VMH appears to be linked to metabolic and behavioral responses(Chan and Sherwin, 2013; Morton et al., 2006), and specifically to the control of thermogenesis and BAT modulation(Kim et al., 2011; Lopez et al., 2010; Martinez de Morentin et al., 2014). Moreover, a role for the VMH in circadian control has been suggested (Egawa et al., 1991; Kiba et al., 2010; Nagai et al., 1983; Orozco-Solis et al., 2015), though understanding the function of the endogenous clock within the VMH has been lacking. By targeted ablation of *Bmal1* in the SF1-neurons we have demonstrated that the VMH circadian clock controls energy expenditure through the modulation of the circadian thermogenic activity of the BAT. Importantly, disruption of the VMH clock does not affect the circadian oscillations in the SCN and other circadian functions (Figure 1).

Accumulating evidence illustrates the role of the BAT on energy expenditure by heat production in both humans and rodents (Lowell et al., 1993; Nedergaard and Cannon, 2014). Also, an inverse correlation between the appearance of brown and beige adipocytes and the development of obesity and type 2 diabetes in humans is well known(Enerback, 2010). This notion is in keeping with the observation that increased temperature mediated by BAT activity inversely correlates with body weight. Importantly, the BAT on the *Sf1-Cre*, *Bmal1*$^{loxP/loxP}$ mice is mainly over-activated during the dark period, implying the presence of a circadian component responsible for the observed effects. Notably, there is no major clock disruption in the BAT and liver of the *Sf1-Cre*, *Bmal1*$^{loxP/loxP}$ mice, suggesting that the over-activation during the active phase of BAT is provoked by external circadian inputs. We have demonstrated that this effect is indeed under sympathetic control (Figure 5). This parallels the notions that the BAT is densely innervated by sympathetic efferents (Bartness et al., 2010) and that the sympathetic system controls circadian peripheral functions, including the cyclic fluctuation of epinephrine(Gamble et al., 2014; Linsell et al., 1985). Indeed, we have shown that over-activation of BAT in the *Sf1-Cre*, *Bmal1*$^{loxP/loxP}$ depends on the adrenergic receptor (Figures 5A-5C), in keeping with a proposed role of the SNS in the synchronization of peripheral clocks by the central pacemaker (Buijs and Kalsbeek, 2001).

Food restriction acts as a powerful metabolic zeitgeber in peripheral tissues and hypothalamic nuclei (Stephan, 2002). Importantly, *Sf1-Cre,Bmal1*$^{loxP/loxP}$ mice exposed to nutrients as zeitgeber (food restriction under DD) did not completely resynchronizes their metabolic rate to the food restricted period (Figure 6D), in keeping with indications on the

role of the VMH (Kozlov et al., 2007). Importantly, our observations show that the endogenous clock in the VMH has a pivotal role in computing zeitgeber information from the SCN and nutrient inputs from the periphery to generate circadian basal respiratory rate in the BAT.

Recent results using mice with total ablation of the *Rev-erbα* gene show impaired regulation of circadian rhythms in BAT by inhibition of the thermogenesis during the inactive (light) period leading to impaired responses to cold stress during this circadian time (Gerhart-Hines et al., 2013). We have demonstrated that disruption of the clock specifically in the Sf1 neurons of the VMH alters the circadian BAT activity without affecting the BAT's endogenous clock, in conditions near thermoneutrality and independently of the mice activity. Indeed, at thermoneutral conditions the contribution of energy expenditure by spontaneous activity is only ~10%, being virtually undetectable at lower temperatures, in spite of the increase of energy expenditure as an adaptative response (Virtue et al., 2012). Therefore, our results suggest that at thermoneutral conditions the circadian oscillation of thermogenesis is controlled by two main components: the intrinsic circadian clock in the BAT, and the hypothalamic circadian control from the synaptic efferents of the SNS. The presence of direct synaptic connections between the VMH and BAT remains to be demonstrated (Cannon and Nedergaard, 2004). However, the preoptic area of the hypothalamus (POA) through the raphe pallidus (RP) elicits SNS's stimuli to the BAT, modulating thermogenic responses (Yoshida et al., 2003). Importantly, the POA interacts with the VMH, probably through GABAergic efferents towards the VMH (Cannon and Nedergaard, 2004), and together modulate BAT activity (Cannon and Nedergaard, 2004). Hence, an intriguing possibility would be that the VMH indirectly communicates with the BAT through the POA and the RP, acting as an integrator of metabolic information. The contribution of the SNS might be crucial for both basal and acute responses, including the circadian control of metabolism from the VMH (Figure 7).

Here, we have demonstrated the critical role of the core clock protein BMAL1 in the SF1-neurons of the VMH in the control of circadian energy expenditure through the SNS, particularly in the control of thermogenesis by the BAT (Figure 7). Further studies will be aimed at deciphering the cellular mechanisms and signaling circuits within neurons implicated in circadian responses, possibly offering opportunities to design strategies for alternative chronoterapies. In addition to possible pharmacological approaches, these could be based on the modulation of hypothalamic clocks by external zeitgebers such as light, food restriction and even restricted cold exposition so to trigger the catabolic capacity of peripheral tissues.

Experimental Procedures

Animals

Animals and protocols used in this study were reviewed and approved by the Institutional Animal Care and Use Committee of the University of California, Irvine. To generate animals with *Bmal1* ablation in SF1 neurons, *Bmal1*$^{loxP/loxP}$ mice (Jackson laboratory, strain B6.129S4(Cg)-*Arntl*^{tm1Weit}/J) were crossed with *Sf1*-Cre mice (Storch et al., 2007). To verify the genotype, tails were cut and the DNA was extracted by alkaline method and the

DNA was amplified by PCR. Animals were individually housed with ad-libitum food access at 24–25 °C room temperature.

Nuclei dissection

The micro-dissection of the SCN, VMH and HIPP was carried as previously described (Orozco-Solis et al., 2015). In the case of the DNA extraction, the dissected nuclei were placed in 20 μl of alkaline lysis buffer (25mM NaOH, 0.2 mM EDTA, pH~12), and incubated at 90 °C in a standard thermo-cycler. Then 2 μl of DNA was used for PCR amplification and resolved in 2% agarose gel. Total RNA was extracted from each sample using TRIzol (Invitrogen) following manufacturer's instructions scaled to 1:10. Total RNA was resuspended in 10 μl of RNAse free water and quantified. cDNA was synthesized from 200 ng of RNA using the cDNA Synthesis kit i-Script (Bio-Rad). The obtained cDNA was then diluted 1:10 and 5 μl was used as template for RT-PCR amplification using SYBR Green (Bio-Rad). The primers used for the amplification are presented (Table S5).

Immunofluorescence

Brains were extracted, frozen in dry-ice and stocked at −80C. Then, brains were sectioned in a cryostat (Leica CM1950) in serial coronal section at 30 μm and 15 μm thick, and the 15 μm sections were mounted in microscope slides and stocked at −80 C until inmunofluorescence. The 30 μm sections were Nissl stained. The selected 15 μm sections were fixed 20 min in 4% PFA-PBS and washed in PBS followed by 3 washes in TBS. The brains slides were permeabilized in 0.3% triton-TBS incubated 1 hr in 1X blocker (BSA in TBS, Pierce). The slides were incubated 24 hrs at 4°C with the primary antibody anti-BMAL1 (sc-48790, Santa Cruz) diluted 1:100 during 24 hrs at 4°C. Then the slides were washed 3 times and incubated with the secondary antibody alexa 400 (Invitrogen) 1:500 during 1 hr at room temperature. The slides were washed 3 times and incubated with DRAQ 1:1000 15 min and washed 2 and mounted with Vector Shield. The brains were observed in a confocal microscope Leyca. The images were analyzed with the ImageJ software (http://imagej.nih.gov/ij/). For the BAT immunofluorescence, the tissue was sectioned in 20 μM thick and mounted in the slides, following the above protocol. The primary antibody anti-mtCO1 (ab14705, Abcam) 1:2000.

Metabolic parameters

VO2 , VCO2 and EE was measured by indirect calorimetry using negative-flow system cages (Columbus Instruments). Rectal temperature was measured with the Thermcouple Meter (WD-35627-00, Kent Scientific). Thermographic temperature was obtained with the infrared camera FLIRi7 (FLIR Systems). Free fatty acid content was obtained with the Triglyceride Colorimetric Assay Kit (Cayman Chemical # 10010303) following the recommended protocol. The mitochondrial DNA (mtDNA) was determined by analyzing the abundance of the mitochondrial gene COX1 relative to the nuclear gene 18S. Total DNA was isolated using the DNEasy Tissue kit (Qiagen). The DNA was sonicated during 10 min and quantified. 10-100ng of total DNA was subjected to QPCR using Sybr Green Chemistry. The β-oxidation was performed "*ex-vivo*". The dissected BAT was weighted and samples were minced and homogenized in 300 μl of homogenization buffer (DMEM, 1mM pyruvate, 1% BSA free fatty acid, 0.5 mM oleate) at 4°C. Then, 5 μl of oleic acid [^{14}C] 100μC/ml was

added, and these lysates were incubated 2 hrs at 37°C. Eppendorf tubes were prepared containing small pieces of whatman paper (wet with 20 µl of NaOH 3M) in the cap of the tube, and 150µl of 70% perchloric acid inside the tube. Lysates were added to the prepared tubes and incubated 1 hr at 37°C. The filter discs were transferred to the scintillation vial and measured in a scintillation counter.

MitoTracker staining

About 30 mg of BAT was lightly minced in small pieces and deposited in 100 µl of DMEM without serum. Then 100 µl of staining solution 500 nM Orange CM-H2TMRos (M-7511 Life Technologies) in DMEM. The tissue was incubated at 37°C 20–30 min, washed 2 times with DMEM, and fixed 10 min at 37°C in formaldehyde 3.7%-DMEM. The tissue was washed 2 times with PBS, incubated 15 min at 37°C in PBS-DRAQ5 (1:1000), washed with PBS and mounted with Vectashield. Images were obtained with a confocal microscope (Leica SP5), using a 60X oil objective.

SR59230A administration

Two groups of 5 months old (n=8) were injected at ZT 16 with 100 µl solution in a dose of 3 mg/kg of SR59230A (ab142536, Abcam) or saline as experimental control. After 1.5 hrs post injection mice were sacrificed and the BAT was immediately analyzed to determine *ex-vivo* β-oxidation. BAT samples were frozen at −80C for subsequent RNA extraction.

Western analyses

The tissue was homogenized in modified RIPA buffer (50 mM Tris-HCl pH 8.0, 150 mM NaCl, 5 mM EDTA, 15 mM $MgCl_2$, 1%NP-40) supplemented with protease and phosphatase inhibitor cocktails. About 20 µg of protein extracts was electrophoresed on SDS-PAGE gels and transferred to nitrocellulose membranes. The membranes were incubated 12 hrs at 4°C with the primary antibodies, anti-mtCO1 (ab14705, Abcam) 1:2000 and anti-Pparα (sc-9000, Santa Cruz Biotechnology) 1:500. The membranes were visualized by peroxidase conjugated secondary antibodies and ECL chemiluminescent substrate.

Circadian behavior

Locomotor activity was detected using optical beam motion detection (Philips Respironics). Data was collected using the Minimitter VitalView 5.0. The *tau* values was calculated by obtaining the slopes at the onset of the free activity component, and then computed using Clocklab software (Actimetrics), by the least-squares fits method, and by X^2 periodogram method.

Data analysis

Experimental results are expressed as means ± SEM. Unpaired Student's t-test was used to compare two groups from different genotype. To compare the differences between ZT or days and genotype, data was analyzed by two way-ANOVA followed by Bonferroni's post-hoc test for multiple comparisons. The data from indirect calorimetry was analyzed by ANCOVA followed by Bonferroni's post hoc test, using the metabolic parameter (heat, VO2

or VCO2) during the LD period as a dependent variable, genotype as a factor and body weight as a covariate. Circadian parameters were obtained using the Time Series Analysis Seriel Cosinor 6.3 (http://www.euroestech.com/). First, we determined the correct distribution (data interdependency and normal distribution) for each time series data by lag plots/Q-test and normal probability plots/K-S test, and then we calculated the acrophase and amplitude by the Cosinor method using a period of 24 h. The values for each animal and each gene were averaged and analyzed statistically.

Histological staining

Frozen BAT and WAT were sliced at 10 μm thick in a Leica CM195 cryostat, and mounted in the slides. The slides were stained with Hematoxylin and Eosin (H&E) stain and/or Oil-Red-Oil stain as previously described.

Supplementary Material

Refer to Web version on PubMed Central for supplementary material.

Acknowledgments

We thank all members of the Sassone-Corsi laboratory for constructive comments and help. We would also thank Yumay Chen and Ping Wang for helpful assistance using the Seahorse analyzer, and Sherry Dilag for her technical assistance on histological staining. R.O.-S. was supported by a fellowship from the Government of Mexico (CONACYT) and by the Della Martin Foundation; L. A.-A. was supported by a long-term EMBO post-doctoral fellowship. This study was supported by funds of the National Institute of Health, the Merieux Fondation, and INSERM (Institut National de la Sante et Recherche Medicale, France).

BIBLIOGRAPHY

Amir S. Intra-ventromedial hypothalamic injection of glutamate stimulates brown adipose tissue thermogenesis in the rat. Brain Res. 1990; 511:341–344. [PubMed: 1970749]

Asher G, Sassone-Corsi P. Time for Food: The Intimate Interplay between Nutrition, Metabolism, and the Circadian Clock. Cell. 2015; 161:84–92. [PubMed: 25815987]

Barbera MJ, Schluter A, Pedraza N, Iglesias R, Villarroya F, Giralt M. Peroxisome proliferator-activated receptor alpha activates transcription of the brown fat uncoupling protein-1 gene. A link between regulation of the thermogenic and lipid oxidation pathways in the brown fat cell. J Biol Chem. 2001; 276:1486–1493. [PubMed: 11050084]

Bartness TJ, Vaughan CH, Song CK. Sympathetic and sensory innervation of brown adipose tissue. Int J Obes. 2010; 34:S36–S42.

Bexis S, Docherty JR. Role of α1- and β3-adrenoceptors in the modulation by SR59230A of the effects of MDMA on body temperature in the mouse. British Journal of Pharmacology. 2009; 158:259–266. [PubMed: 19422394]

Bingham NC, Anderson KK, Reuter AL, Stallings NR, Parker KL. Selective loss of leptin receptors in the ventromedial hypothalamic nucleus results in increased adiposity and a metabolic syndrome. Endocrinology. 2008; 149:2138–2148. [PubMed: 18258679]

Buijs RM, Kalsbeek A. Hypothalamic integration of central and peripheral clocks. Nat Rev Neurosci. 2001; 2:521–526. [PubMed: 11433377]

Buxton OM, Cain SW, O'Connor SP, Porter JH, Duffy JF, Wang W, Czeisler CA, Shea SA. Adverse Metabolic Consequences in Humans of Prolonged Sleep Restriction Combined with Circadian Disruption. Sci Transl Med. 2012; 4:129ra143.

Cannon B, Nedergaard J. Brown adipose tissue: function and physiological significance. Physiological reviews. 2004; 84:277–359. [PubMed: 14715917]

Cederberg A, Gronning LM, Ahren B, Tasken K, Carlsson P, Enerback S. FOXC2 is a winged helix gene that counteracts obesity, hypertriglyceridemia, and diet-induced insulin resistance. Cell. 2001; 106:563–573. [PubMed: 11551504]

Chaix A, Zarrinpar A, Miu P, Panda S. Time-Restricted Feeding Is a Preventative and Therapeutic Intervention against Diverse Nutritional Challenges. Cell Metab. 20:991–1005.

Chan O, Sherwin R. Influence of VMH fuel sensing on hypoglycemic responses. Trends in Endocrinology & Metabolism. 2013; 24:616–624. [PubMed: 24063974]

Choi Y-H, Fujikawa T, Lee J, Reuter A, Kim KW. Revisiting the Ventral Medial Nucleus of the Hypothalamus: The Roles of SF-1 Neurons in Energy Homeostasis. Frontiers in neuroscience. 2013; 7:71. [PubMed: 23675313]

Cypess AM, Weiner LS, Roberts-Toler C, Franquet Elia E, Kessler SH, Kahn PA, English J, Chatman K, Trauger SA, Doria A, Kolodny GM. Activation of human brown adipose tissue by a beta3-adrenergic receptor agonist. Cell Metab. 2015; 21:33–38. [PubMed: 25565203]

Dhillon H, Zigman JM, Ye C, Lee CE, McGovern RA, Tang V, Kenny CD, Christiansen LM, White RD, Edelstein EA, Coppari R, Balthasar N, Cowley MA, Chua S Jr, Elmquist JK, Lowell BB. Leptin directly activates SF1 neurons in the VMH, and this action by leptin is required for normal body-weight homeostasis. Neuron. 2006; 49:191–203. [PubMed: 16423694]

Eckel-Mahan K, Sassone-Corsi P. Metabolism and the circadian clock converge. Physiological reviews. 2013; 93:107–135. [PubMed: 23303907]

Eckel-Mahan KL, Patel VR, de Mateo S, Orozco-Solis R, Ceglia NJ, Sahar S, Dilag-Penilla SA, Dyar KA, Baldi P, Sassone-Corsi P. Reprogramming of the circadian clock by nutritional challenge. Cell. 2013; 155:1464–1478. [PubMed: 24360271]

Egawa M, Inoue S, Sato S, Takamura Y, Murakami N, Takahashi K. Restoration of circadian corticosterone rhythm in ventromedial hypothalamic lesioned rats. Neuroendocrinology. 1991; 53:543–548. [PubMed: 1876233]

Enerback S. Human brown adipose tissue. Cell Metab. 2010; 11:248–252. [PubMed: 20374955]

Fan W, Evans R. PPARs and ERRs: molecular mediators of mitochondrial metabolism. Curr Opin Cell Biol. 2014; 33C:49–54.

Gamble KL, Berry R, Frank SJ, Young ME. Circadian clock control of endocrine factors. Nat Rev Endocrinol. 2014; 10:466–475. [PubMed: 24863387]

Gerhart-Hines Z, Feng D, Emmett MJ, Everett LJ, Loro E, Briggs ER, Bugge A, Hou C, Ferrara C, Seale P, Pryma DA, Khurana TS, Lazar MA. The nuclear receptor Rev-erb[agr] controls circadian thermogenic plasticity. Nature. 2013; 503:410–413. [PubMed: 24162845]

Halvorson I, Gregor L, Thornhill JA. Brown adipose tissue thermogenesis is activated by electrical and chemical (L-glutamate) stimulation of the ventromedial hypothalamic nucleus in cold-acclimated rats. Brain research. 1990; 522:76–82. [PubMed: 2224517]

Harms M, Seale P. Brown and beige fat: development, function and therapeutic potential. Nat Med. 2013; 19:1252–1263. [PubMed: 24100998]

Honma, K-i, Honma, S. The SCN-independent clocks, methamphetamine and food restriction. The European journal of neuroscience. 2009; 30:1707–1717. [PubMed: 19878275]

Janich P, Pascual G, Merlos-Suarez A, Batlle E, Ripperger J, Albrecht U, Cheng H-YM, Obrietan K, Di Croce L, Benitah SA. The circadian molecular clock creates epidermal stem cell heterogeneity. Nature. 2011; 480:209–214. [PubMed: 22080954]

Johnson BP, Walisser JA, Liu Y, Shen AL, McDearmon EL, Moran SM, McIntosh BE, Vollrath AL, Schook AC, Takahashi JS, Bradfield CA. Hepatocyte circadian clock controls acetaminophen bioactivation through NADPH-cytochrome P450 oxidoreductase. Proceedings of the National Academy of Sciences. 2014; 111:18757–18762.

Kajimura S, Seale P, Spiegelman BM. Transcriptional Control of Brown Fat Development. Cell Metab. 2010; 11:257–262. [PubMed: 20374957]

Kiba T, Kintaka Y, Suzuki Y, Ishizuka N, Ishigaki Y, Inoue S. VMH lesions downregulate the expression of Per2 gene in the pancreas in the rat. Neuroscience letters. 2010; 471:148–151. [PubMed: 20096750]

Kim KW, Donato J Jr, Berglund ED, Choi Y-H, Kohno D, Elias CF, DePinho RA, Elmquist JK. FOXO1 in the ventromedial hypothalamus regulates energy balance. The Journal of Clinical Investigation. 2012; 122:2578–2589. [PubMed: 22653058]

Kim KW, Zhao L, Donato J Jr, Kohno D, Xu Y, Elias CF, Lee C, Parker KL, Elmquist JK. Steroidogenic factor 1 directs programs regulating diet-induced thermogenesis and leptin action in the ventral medial hypothalamic nucleus. Proceedings of the National Academy of Sciences of the United States of America. 2011; 108:10673–10678. [PubMed: 21636788]

Klockener T, Hess S, Belgardt BF, Paeger L, Verhagen LAW, Husch A, Sohn J-W, Hampel B, Dhillon H, Zigman JM, Lowell BB, Williams KW, Elmquist JK, Horvath TL, Kloppenburg P, Bruning JC. High-fat feeding promotes obesity via insulin receptor/PI3K-dependent inhibition of SF-1 VMH neurons. Nat Neurosci. 2011; 14:911–918. [PubMed: 21642975]

Kozlov SV, Bogenpohl JW, Howell MP, Wevrick R, Panda S, Hogenesch JB, Muglia LJ, Van Gelder RN, Herzog ED, Stewart CL. The imprinted gene Magel2 regulates normal circadian output. Nat Genet. 2007; 39:1266–1272. [PubMed: 17893678]

Liew CW, Boucher J, Cheong JK, Vernochet C, Koh H-J, Mallol C, Townsend K, Langin D, Kawamori D, Hu J, Tseng Y-H, Hellerstein MK, Farmer SR, Goodyear L, Doria A, Bluher M, Hsu SIH, Kulkarni RN. Ablation of TRIP-Br2, a regulator of fat lipolysis, thermogenesis and oxidative metabolism, prevents diet-induced obesity and insulin resistance. Nat Med. 2013; 19:217–226. [PubMed: 23291629]

Linsell CR, Lightman SL, Mullen PE, Brown MJ, Causon RC. Circadian rhythms of epinephrine and norepinephrine in man. The Journal of clinical endocrinology and metabolism. 1985; 60:1210–1215. [PubMed: 3998066]

Lopez M, Varela L, Vazquez MJ, Rodriguez-Cuenca S, Gonzalez CR, Velagapudi VR, Morgan DA, Schoenmakers E, Agassandian K, Lage R, Martinez de Morentin PB, Tovar S, Nogueiras R, Carling D, Lelliott C, Gallego R, Oresic M, Chatterjee K, Saha AK, Rahmouni K, Dieguez C, Vidal-Puig A. Hypothalamic AMPK and fatty acid metabolism mediate thyroid regulation of energy balance. Nature medicine. 2010; 16:1001–1008.

Lowell BB, V SS, Hamann A, Lawitts JA, Himms-Hagen J, Boyer BB, Kozak LP, Flier JS. Development of obesity in transgenic mice after genetic ablation of brown adipose tissue. Nature. 1993; 366:740–742. [PubMed: 8264795]

Mandard S, Muller M, Kersten S. Peroxisome proliferator-activated receptor alpha target genes. Cell Mol Life Sci. 2004; 61:393–416. [PubMed: 14999402]

Martinez de Morentin PB, Gonzalez-Garcia I, Martins L, Lage R, Fernandez-Mallo D, Martinez-Sanchez N, Ruiz-Pino F, Liu J, Morgan DA, Pinilla L, Gallego R, Saha AK, Kalsbeek A, Fliers E, Bisschop PH, Dieguez C, Nogueiras R, Rahmouni K, Tena-Sempere M, Lopez M. Estradiol regulates brown adipose tissue thermogenesis via hypothalamic AMPK. Cell Metab. 2014; 20:41–53. [PubMed: 24856932]

Masri S, Sassone-Corsi P. The circadian clock: a framework linking metabolism, epigenetics and neuronal function. Nat Rev Neurosci. 2013; 14:69–75. [PubMed: 23187814]

Minokoshi Y, Saito M, Shimazu T. Sympathetic denervation impairs responses of brown adipose tissue to VMH stimulation. Am. J. Physiol. 1986; 251:R1005–R1008. [PubMed: 3777207]

Morrison SF, Madden CJ, Tupone D. Central neural regulation of brown adipose tissue thermogenesis and energy expenditure. Cell Metab. 2014; 19:741–756. [PubMed: 24630813]

Morton GJ, Cummings DE, Baskin DG, Barsh GS, Schwartz MW. Central nervous system control of food intake and body weight. Nature. 2006; 443:289–295. [PubMed: 16988703]

Myers MG Jr, Olson DP. Central nervous system control of metabolism. Nature. 2012; 491:357–363. [PubMed: 23151578]

Nagai K, Inoue S, Nakagawa H. Reciprocal changes in gluconeogenic enzyme activity in liver and kidney by VMH lesion. The American journal of physiology. 1983; 245:E14–E18. [PubMed: 6869526]

Nedergaard J, Cannon B. The Browning of White Adipose Tissue: Some Burning Issues. Cell Metab. 2014; 20:396–407. [PubMed: 25127354]

Ootsuka Y, Kulasekara K, de Menezes RC, Blessing WW. SR59230A, a beta-3 adrenoceptor antagonist, inhibits ultradian brown adipose tissue thermogenesis and interrupts associated episodic brain and body heating. 2011

Orozco-Solis R, Ramadori G, Coppari R, Sassone-Corsi P. SIRT1 Relays Nutritional Inputs to the Circadian Clock Through the Sf1 Neurons of the Ventromedial Hypothalamus. Endocrinology. 2015; 156:2174–2184. [PubMed: 25763637]

Orozco-Solis R, Sassone-Corsi P. Circadian clock: linking epigenetics to aging. Current Opinion in Genetics & Development. 2014; 26:66–72. [PubMed: 25033025]

Özbudak EM, Tassy O, Pourquié O. Spatiotemporal compartmentalization of key physiological processes during muscle precursor differentiation. Proceedings of the National Academy of Sciences. 2010; 107:4224–4229.

Paschos GK, Ibrahim S, Song W-L, Kunieda T, Grant G, Reyes TM, Bradfield CA, Vaughan CH, Eiden M, Masoodi M, Griffin JL, Wang F, Lawson JA, FitzGerald GA. Obesity in mice with adipocyte-specific deletion of clock component Arntl. Nat Med. 2012; 18:1768–1777. [PubMed: 23142819]

Perkins MN, Rothwell NJ, Stock MJ, Stone TW. Activation of brown adipose tissue thermogenesis by the ventromedial hypothalamus. Nature. 1981; 289:401–402. [PubMed: 7464907]

Plaisier CL, Bennett BJ, He A, Guan B, Lusis AJ, Reue K, Vergnes L. Zbtb16 has a role in brown adipocyte bioenergetics. Nutrition and Diabetes. 2012; 2:e46.

Ramadori G, Fujikawa T, Anderson J, Berglund ED, Frazao R, Michan S, Vianna CR, Sinclair DA, Elias CF, Coppari R. SIRT1 deacetylase in SF1 neurons protects against metabolic imbalance. Cell Metab. 2011; 14:301–312. [PubMed: 21907137]

Ruan HB, Dietrich MO, Liu ZW, Zimmer MR, Li MD, Singh JP, Zhang K, Yin R, Wu J, Horvath TL, Yang X. O-GlcNAc Transferase Enables AgRP Neurons to Suppress Browning of White Fat. Cell. 2014; 159:306–317. [PubMed: 25303527]

Schulz TJ, Huang P, Huang TL, Xue R, McDougall LE, Townsend KL, Cypess AM, Mishina Y, Gussoni E, Tseng Y-H. Brown-fat paucity due to impaired BMP signalling induces compensatory browning of white fat. Nature. 2013; 495:379–383. [PubMed: 23485971]

Shiromani PJ, Xu M, Winston EM, Shiromani SN, Gerashchenko D, Weaver DR. Sleep rhythmicity and homeostasis in mice with targeted disruption of mPeriod genes. 2004

Stephan FK. The “Other” Circadian System: Food as a Zeitgeber. Journal of Biological Rhythms. 2002; 17:284–292. [PubMed: 12164245]

Storch KF, Paz C, Signorovitch J, Raviola E, Pawlyk B, Li T, Weitz CJ. Intrinsic circadian clock of the mammalian retina: importance for retinal processing of visual information. Cell. 2007; 130:730–741. [PubMed: 17719549]

Stuart JA, Brindle KM, Harper JA, Brand MD. Mitochondrial proton leak and the uncoupling proteins. Journal of bioenergetics and biomembranes. 1999; 31:517–525. [PubMed: 10653479]

Virtue S, Even P, Vidal-Puig A. Below Thermoneutrality, Changes in Activity Do Not Drive Changes in Total Daily Energy Expenditure between Groups of Mice. Cell Metabolism. 2012; 16:665–671. [PubMed: 23140644]

Virtue S, Vidal-Puig A. Assessment of brown adipose tissue function. Frontiers in Physiology. 2013; 4:128. [PubMed: 23760815]

Wu Z, Puigserver P, Andersson U, Zhang C, Adelmant G, Mootha V, Troy A, Cinti S, Lowell B, Scarpulla RC, Spiegelman BM. Mechanisms Controlling Mitochondrial Biogenesis and Respiration through the Thermogenic Coactivator PGC-1. Cell. 1999; 98:115–124. [PubMed: 10412986]

Yadav VK, Oury F, Suda N, Liu Z-W, Gao X-B, Confavreux C, Klemenhagen KC, Tanaka KF, Gingrich JA, Guo XE, Tecott LH, Mann JJ, Hen R, Horvath TL, Karsenty G. A Serotonin-Dependent Mechanism Explains the Leptin Regulation of Bone Mass, Appetite, and Energy Expenditure. Cell. 2009; 138:976–989. [PubMed: 19737523]

Yoshida K, Nakamura K, Matsumura K, Kanosue K, Konig M, Thiel HJ, Boldogkoi Z, Toth I, Roth J, Gerstberger R, Hubschle T. Neurons of the rat preoptic area and the raphe pallidus nucleus innervating the brown adipose tissue express the prostaglandin E receptor subtype EP3. The European journal of neuroscience. 2003; 18:1848–1860. [PubMed: 14622218]

Yu XX, Lewin DA, Forrest W, Adams SH. Cold elicits the simultaneous induction of fatty acid synthesis and β-oxidation in murine brown adipose tissue: prediction from differential gene expression and confirmation in vivo. The FASEB Journal. 2002; 16:155–168. [PubMed: 11818363]

Zhang R, Dhillon H, Yin H, Yoshimura A, Lowell BB, Maratos-Flier E, Flier JS. Selective Inactivation of Socs3 in SF1 Neurons Improves Glucose Homeostasis without Affecting Body Weight. Endocrinology. 2008; 149:5654–5661. [PubMed: 18669597]

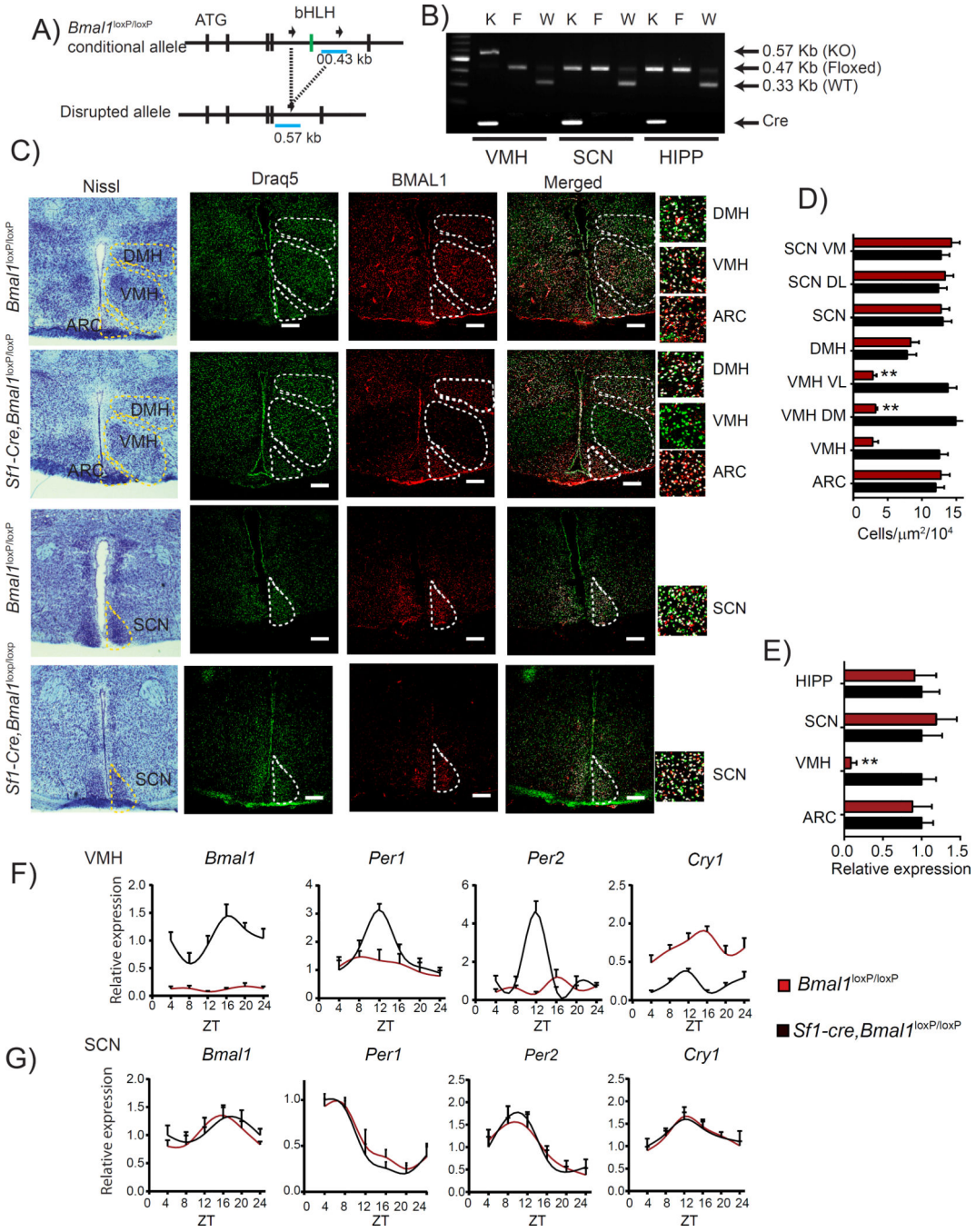

Figure 1. Specific ablation of *Bmal1* in Sf1 neurons of the VMH

A) Schematic illustration showing the conditional flanked region surrounding the basic-helix-loop-helix (bHLH, green) domain of the mouse *Bmal1* locus and the disrupted allele. B) Multiplex PCR genotyping showing the amplified DNA from the VMH, ventromedial hypothalamus; SCN, suprachiasmatic nucleus; HIPP, hippocampus. C) Representative micrographs of brains from Bmal1$^{loxP/loxP}$ and Sf1-Cre;Bmal1$^{loxP/loxP}$ mice. First column shows the Nissl staining to identify the hypothalamic nuclei, second to third columns, confocal micrographs showing Draq5 nuclear stain (green), BMAL1 signal (red) and the

merged micrograph showing the signal in the DMH (dorsomedial hypothalamus), VMH (ventromedial hypothalamus, ARC (arcuate nucleus) and SCN (suprachiasmatic nucleus). D) Counted merged in the different hypothalamic nuclei ARC, VMH, DMH and SCN; (SCN VM, suprachiasmatic nucleus ventro medial part; SCN DL, SCN dorso lateral part; VMH VL, ventromedial hypothalamus ventro lateral part; VMH DM, dorso medial part) E) Relative expression levels of *Bmal1* from micro-dissected nuclei. F) Ablation of *Bmal1* in the Sf1 neurons results in disrupted circadian expression of clock genes *Bmal1, Per1, Per2*, and *Cry1* G) the SCN shows intact expression profiles in both genotypes. (* < 0.05, ** < 0.001 *t*-test) n=4; circadian expression profile, see table S1 (n=4, per time point, * < 0.05, ** < 0.001 Two-way ANOVA followed by Bonferroni's post hoc test). All plots expressed as means ± SEM. Sf1-*Cre*;*Bmal1*$^{loxP/loxP}$, red bars and lines; *Bmal1*$^{loxP/loxP}$, black bars and lines.

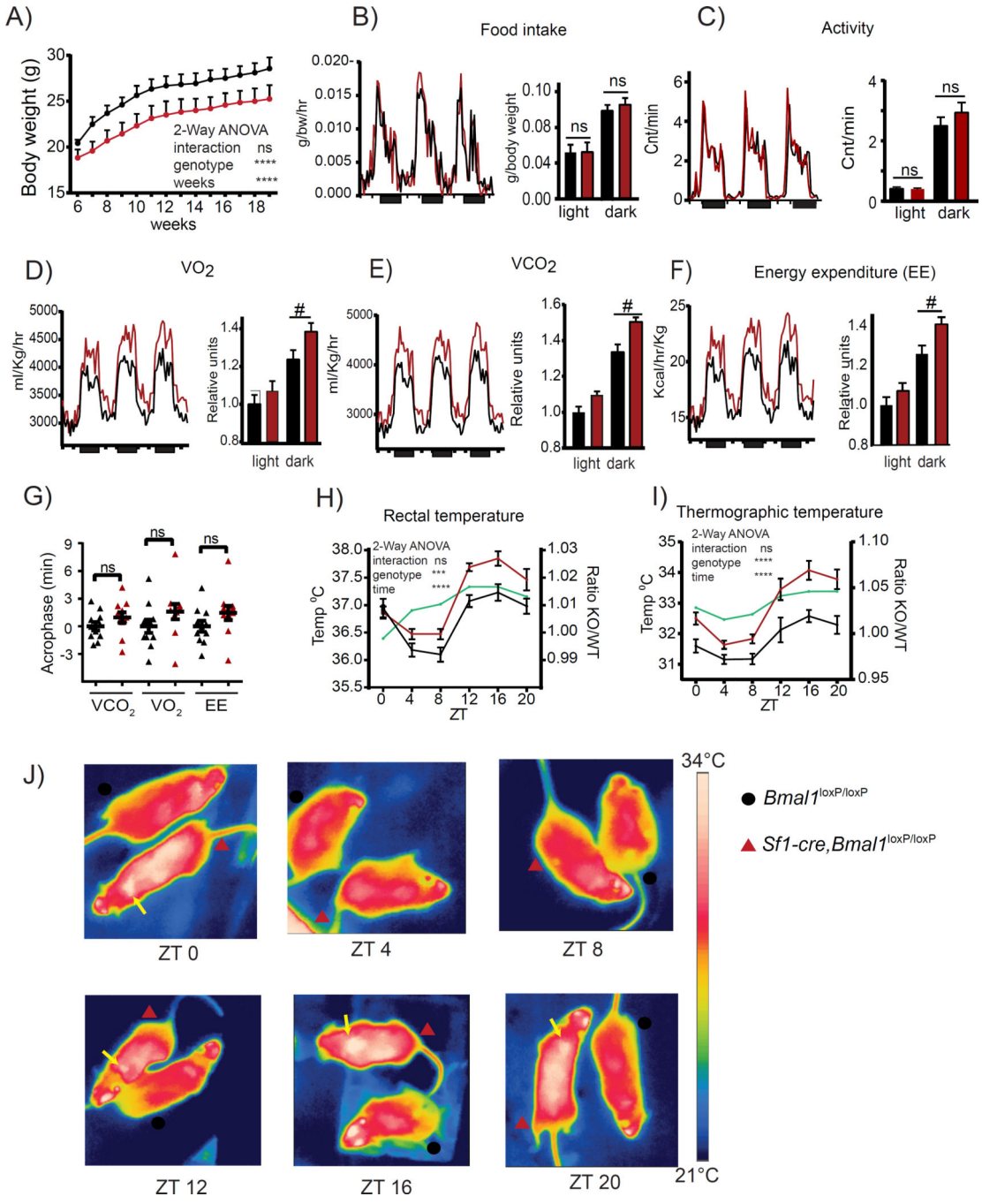

Figure 2. Increased energy expenditure and thermogenic capacity in *Sf1-Cre;Bmal1*$^{loxP/loxP}$ mice

A) Under standard conditions (normal chow, 25°C room temperature) the Sf1-Cre;Bmal1$^{loxP/loxP}$ mice maintain a reduced body weight. B-C) Same levels of food intake and locomotor activity in Sf1- Cre;Bmal1$^{loxP/loxP}$ mice as compared to their *Bmal1*$^{loxP/loxP}$ littermates. D-F) Hourly plots showing the circadian O_2 consumption, CO_2 production and energy expenditure. Bar plots show the respiratory monitoring during the light and dark phase depicting an increment in these parameters during dark phase in the Sf1-Cre;Bmal1$^{loxP/loxP}$ mice. G) Obtained acrophase for the respiratory parameters. H-J)

Circadian rectal and thermographic measurement of body temperature monitored every 4 hrs along the circadian cycle. (* < 0.05, ** < 0.001 Two-way ANOVA followed by Bonferroni's post hoc test, t-test; # < 0.05 ANCOVA). All plots expressed as means ± SEM. n=10 mice per genotype. *Sf1-Cre*;*Bmal1*$^{loxP/loxP}$, red bars and lines; *Bmal1*$^{loxP/loxP}$, black bars and lines.

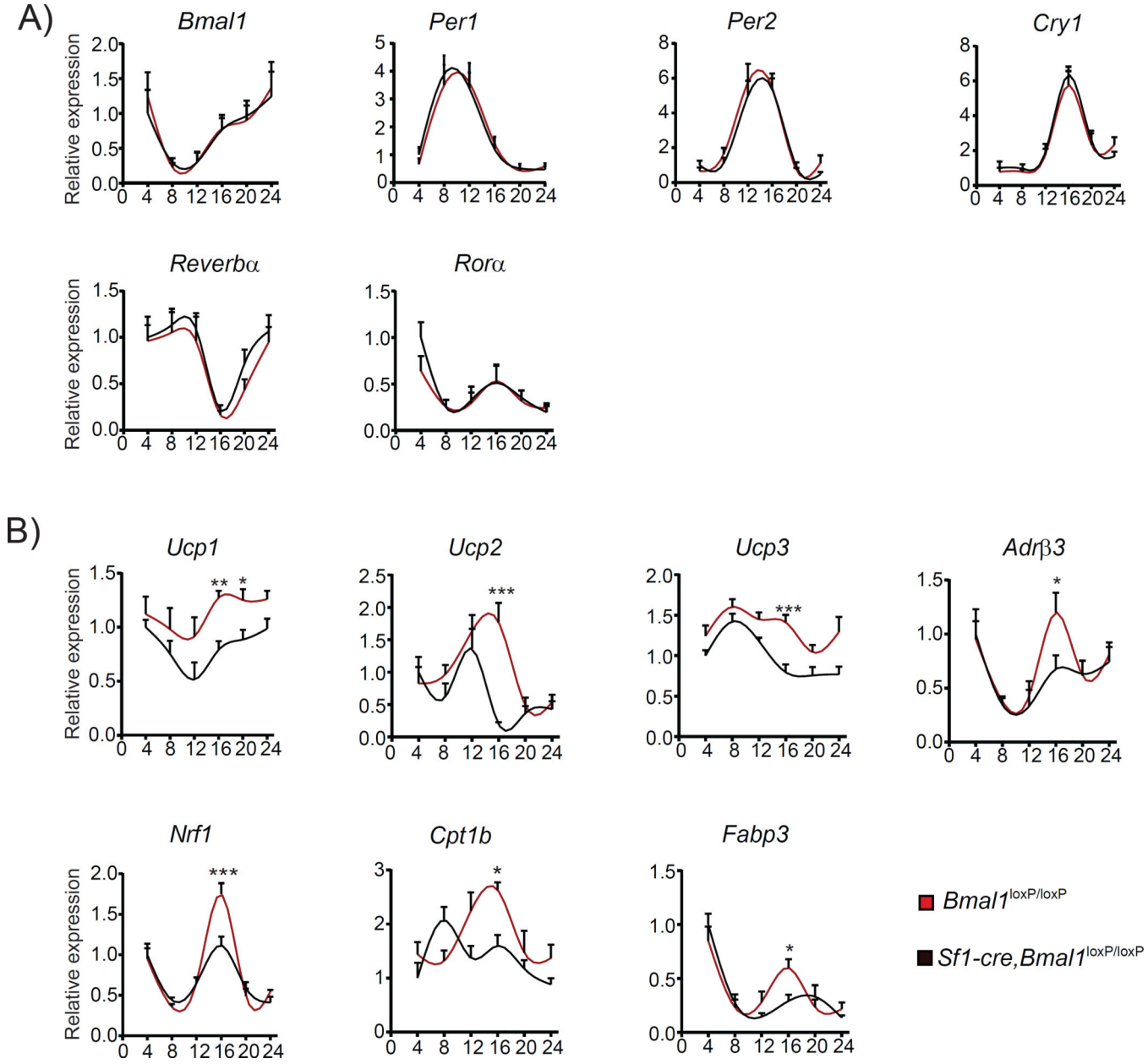

Figure 3. Ablation of *Bmal1* in Sf1-neurons activates the circadian nocturnal expression of thermogenic genes in the BAT

A) Circadian expression of core-clock genes measured every 4 hr along the circadian cycle. No differences were observed between the Sf1-*Cre*;*Bmal1*$^{loxP/loxP}$ mice and the corresponding *Bmal1*$^{loxP/loxP}$ littermates. B) Circadian expression of thermogenic genes showing an increased expression levels during the dark phase in the Sf1-*Cre*;*Bmal1*$^{loxP/loxP}$ mice (* < 0.05, ** < 0.001, *t*-test). All plots expressed as means ± SEM. n=4 per time point. *Sf1-Cre*;*Bmal1*$^{loxP/loxP}$, red lines; *Bmal1*$^{loxP/loxP}$, black lines.

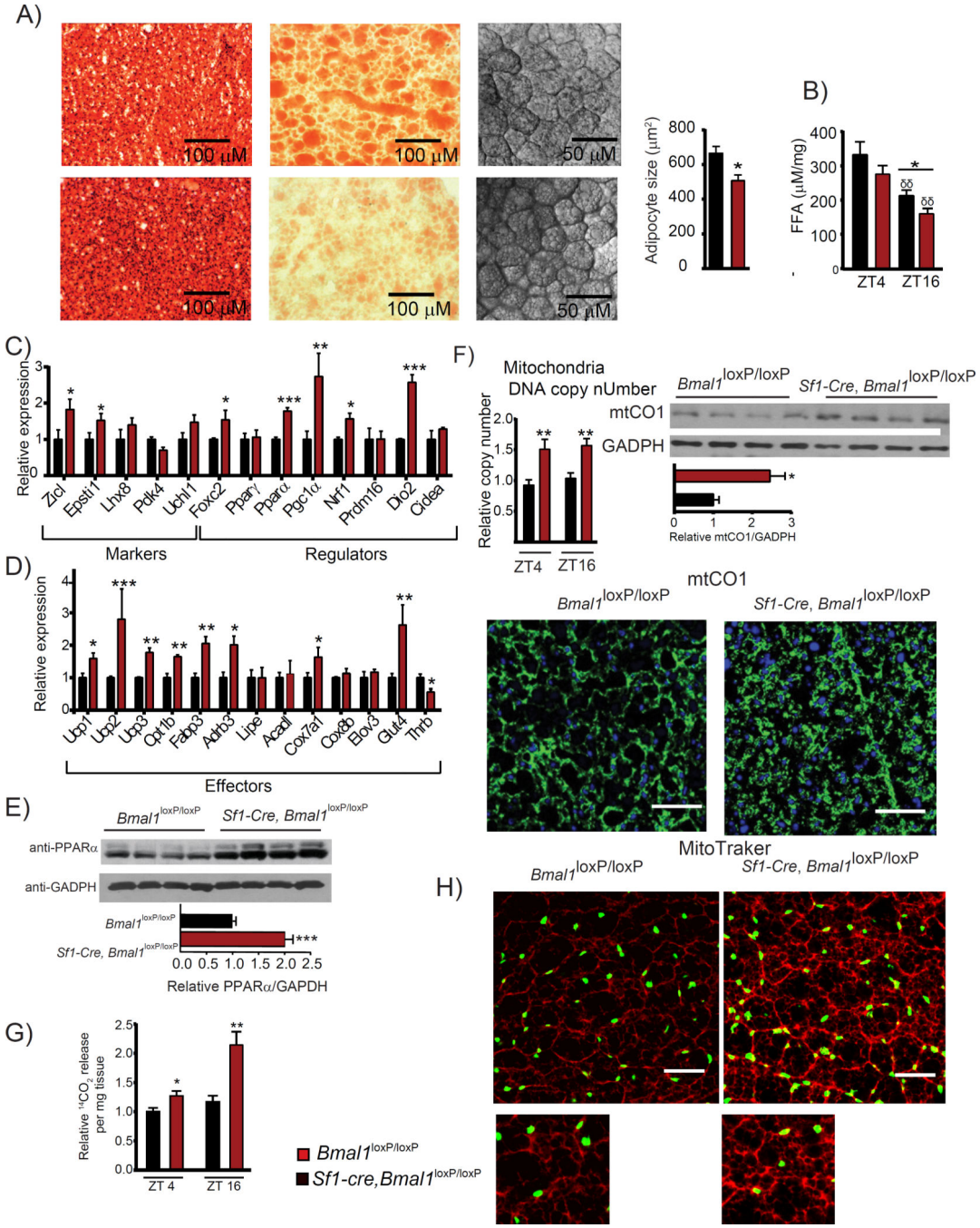

Figure 4. Over-activation of the BAT in *Sf1-Cre;Bmal1*$^{loxP/loxP}$ mice

A) Micrographs showing higher mitochondrial content as revealed by hematoxylin and eosin staining (H&E), lower lipid content by Oil-red-oil (ORO) staining and reduced cellular area (confocal transmission) in the Sf1-*Cre;Bmal1*$^{loxP/loxP}$ mice as compared to *Bmal1*$^{loxP/loxP}$ littermates. B) Sf1-*Cre;Bmal1*$^{loxP/loxP}$ mice display reduced free fatty acid content during the dark period. C-D) Expression of thermogenic genes at ZT 16. E) Expression levels of the PPARα protein. F) Increase in the mitochondrial biogenesis as revealed by mtDNA copy number, mtCO1 protein level revealed by western blot and immunofluorescence (green

signal anti mtCO1, blue signal nuclei). G) Comparison of α-oxidation levels in the light and dark periods. H) Representative micrographs of BAT stained with MitoTraker Orange CM-H_2TMROS revealing mitochondrial oxidative activity. (* < 0.05, ** < 0.001 t-test). All plots expressed as means ± SEM. n=4, per time point. Sf1-, *Cre*;*Bmal1*$^{loxP/loxP}$, red bars; *Bmal1*$^{loxP/loxP}$, black bars.

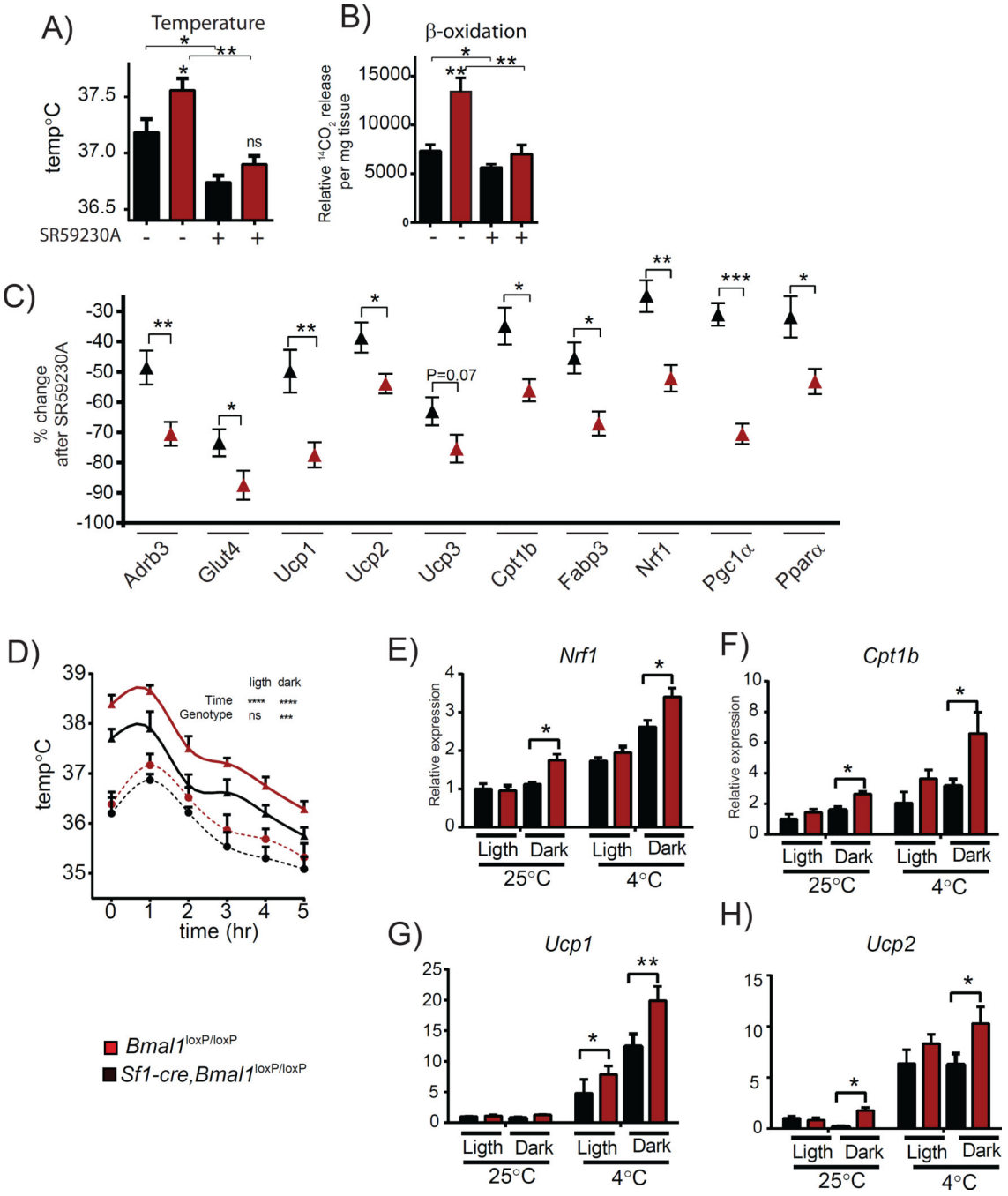

Figure 5. Controls BAT activation by the VMH clock involves efferent signals via sympathetic nervous system

A) Rectal temperature B) β-oxidation rate in response to the ADRB3 antagonist SR59230A. C) Percent change on the expression of thermogenic genes by blocking the ADRB3 D) Time-response on the rectal temperature by exposition of the mice to cold temperature. E-H) Effect of cold exposure on the expression of *Nrf1*, *Cpt1b*, *Ucp1* and *Ucp2* in BAT. Sf1-,Cre;Bmal1$^{loxP/loxP}$, (red symbols);Bmal1$^{loxP/loxP}$, (black symbols). (* < 0.05, ** < 0.001, A, B, D, t-test in; C, Two-way ANOVA followed by Bonferroni's post hoc test). All

plots expressed as means ± SEM. n=5 per group. Sf1-*Cre*;*Bmal1*$^{loxP/loxP}$, red bars, lines and symbols; *Bmal1*$^{loxP/loxP}$, black bars, lines and symbols.

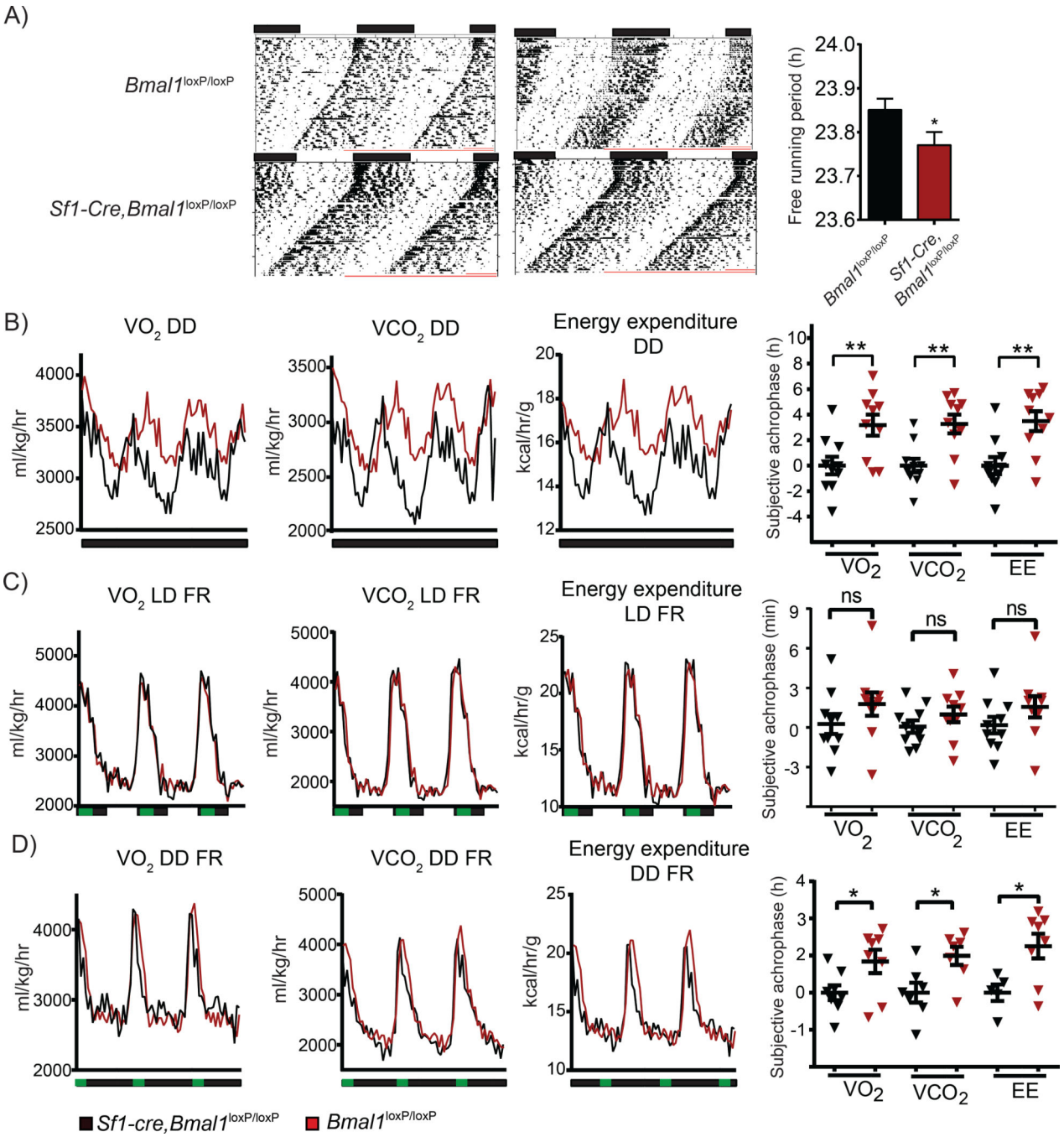

Figure 6. Absence of zeitgebers differentially affects the basal circadian metabolic rate in the *Sf1-Cre;Bmal1*$^{loxP/loxP}$ mice

A) Representative actograms depicting the circadian behavior after 8 days in LD and 50 days DD; right bar plot shows the calculated periods in DD. B) Circadian O_2 consumption, CO_2 production and energy expenditure after 50 days in DD; right, plot depicting the subjective acrophase for the metabolic parameters. C) As in B, in mice exposed in LD and food restriction (FR) from ZT 13-17. D) As in C, in mice exposed to DD and FR. (* < 0.05, *t*-test) n=10 mice per group. Histograms expressed as means ± SEM. Sf1-

Cre;*Bmal1*$^{loxP/loxP}$, red bars, lines and symbols; *Bmal1*$^{loxP/loxP}$, black bars, lines and symbols.

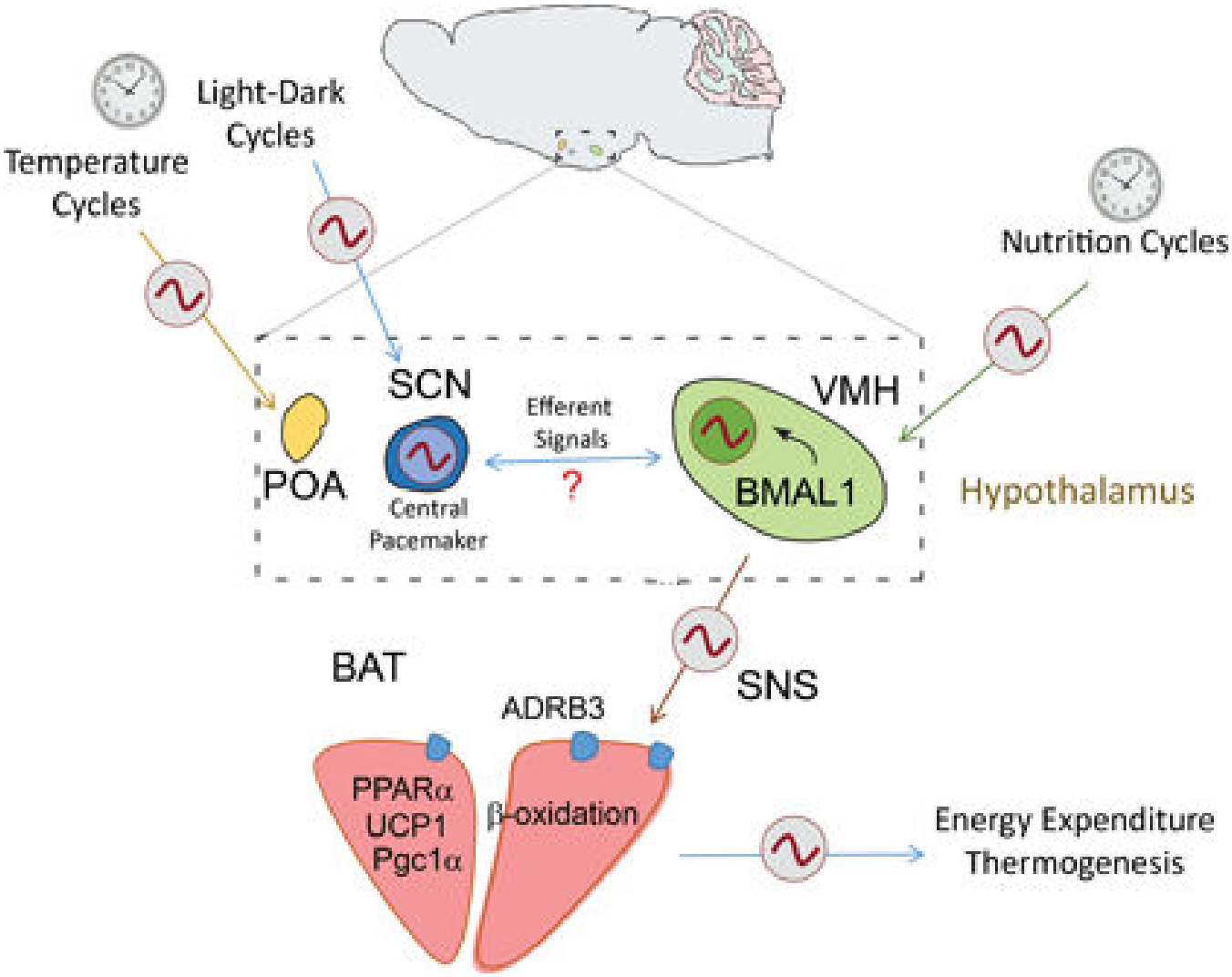

Figure 7. Energy expenditure through the SNS and hypothalamic nuclei can be modulated by external zeitgebers and cold exposure

Recognized external zeitgebers such as the light-dark and circadian feeding cycles synchronize hypothalamic clocks including the SCN and the VMH, which in turns modulates the circadian activity of BAT through the SNS controlling energy balance. Central survival responses to cold exposure might contributes on the circadian modulation of BAT activity, triggered by thermo-sensible hypothalamic nuclei such as the POA.